Measured Adiabatic Effectiveness and Heat Transfer for Blowing From the Tip of a Turbine Blade

J. R. Christophel

E. Couch

K. A. Thole

Mechanical Engineering Department,
Virginia Polytechnic Institute and State University,
Blacksburg, VA 24061

F. J. Cunha

Turbine Durability,
Pratt & Whitney Aircraft Company,
United Technologies Corporation,
East Hartford, CT 06108

The clearance gap between the tip of a turbine blade and the shroud has an inherent leakage flow from the pressure side to the suction side of the blade. This leakage flow of combustion gas and air mixtures leads to severe heat transfer rates on the blade tip of the high-pressure turbine. As the thermal load to the blade increases, blade alloy oxidation and erosion rates increase thereby adversely affecting component life. The subject of this paper is the cooling effectiveness levels and heat transfer coefficients that result from blowing through two holes placed in the forward region of a blade tip. These holes are referred to as dirt purge holes and are generally required for manufacturing purposes and expelling dirt from the coolant flow when operating in sandy environments. Experiments were performed in a linear blade cascade for two tip-gap heights over a range of blowing ratios. Results indicated that the cooling effectiveness was highly dependent on the tip-gap clearance with better cooling achieved at smaller clearances. Also, heat transfer was found to increase with blowing. In considering an overall benefit of cooling from the dirt purge blowing, a large benefit was realized for a smaller tip gap as compared with a larger tip gap. [DOI: 10.1115/1.1811095]

Introduction

The performance of a turbine engine is a strong function of the maximum gas temperature at the rotor inlet. Because turbine airfoils are exposed to hot gas exiting the combustion chamber(s), the materials and cooling methods are of critical importance. Turbine blade designers concentrate heavily on finding better cooling schemes to increase the overall operation life of all turbine airfoils, namely, the high-pressure turbine blades. The clearance between the blade tip and the associated shroud, also known as the blade outer air seal, provides a flow path across the tip that leads to aerodynamic losses and high heat transfer rates along the blade tip. The flow within this clearance gap is driven by a pressure differential between the pressure and suction sides of the blade, but is also affected by the viscous forces as the fluid passes through the gap.

From an operational point of view, engine removals from service are primarily dictated by the spent exhaust gas temperature (EGT) margin caused by deterioration of the high-pressure turbine components. Increased clearance gaps accelerate effects of low-cycle thermal-mechanical fatigue, oxidation, and erosion as a result of increased temperatures in the turbine and decreased EGT margin. In general, tip clearances for large commercial engines are of the order of 0.25 mm, which can reduce the specific fuel consumption by 1% and EGT by 10°C [1]. Improving the blade tip durability can, therefore, produce fuel and maintenance savings over hundreds of millions of dollars per year [1].

The work presented in this paper is on a realistic design for a turbine blade tip consisting of a flat tip, with the exception of a small cavity in which two dirt holes are placed. The location of these holes is a direct consequence of the internal cooling passages within the blade. The purge hole cavity extends only over a small area in the front portion of the blade tip. The function of the dirt purge holes includes the following: (i) purge holes allow centrifugal forces to expel any dirt ingested by the compressor into the turbine rather than clogging the smaller diameter film cooling holes and (ii) purge holes provide a way to support the ceramic core during the lost-wax investment casting of the blade manufacturing process. The dirt purge cavity is present to insure that the purge holes remain open during eventual blade rubbing.

This paper details the film cooling and heat transfer associated with blowing from the dirt purge holes along the tip of a turbine blade. Measurements of adiabatic effectiveness and heat transfer coefficients are studied while varying the tip clearance and mass flux (blowing) ratios.

Relevant Past Studies

The work presented in this paper is concerned with the effects of injecting coolant from the tip of a turbine blade, where the experiments were completed for a stationary, linear cascade. As such, it is important to consider the relevance of past studies to evaluate the effects of the relative motion between the blade tip and outer shroud. It is also relevant to consider tests where tip blowing has been investigated.

Regarding the effects of blade rotation, the first work to address the flow field effects was that of Morphis and Bindon [2] who found that their static-pressure measurements across the blade tip in an annular turbine cascade were not affected by the relative motion at the tip. They concluded that the basic nature of the flow structures remained unchanged with and without relative motion. In contrast, the studies by Tallman and Lakshminarayana [3] and Yaras and Sjölander [4] showed that the leakage flow through the gap was reduced along with the leakage vortex in the case of a moving wall relative to a fixed wall. They attributed this difference to the passage vortex being convected toward the suction surface by the moving wall and postulated that the passage vortex position can alter the driving pressure through the tip gap.

Although there are apparent effects of a moving wall on some of the reported flow field studies, tip heat transfer studies generally indicate relatively minor to nonexistent effects of a moving wall. The reason for this relatively minor effect was first hypothesized by Mayle and Metzger [5], who evaluated the effects of relative motion on the heat transfer in a simple pressure-driven duct flow. They derived and also showed experimentally that for a flow-path length with less than 20 times the clearance gap, the flow can be considered as a developing duct flow. As such, the

Contributed by the International Gas Turbine Institute (IGTI) of THE AMERICAN SOCIETY OF MECHANICAL ENGINEERS for publication in the ASME JOURNAL OF TURBOMACHINERY. Paper presented at the International Gas Turbine and Aeroengine Congress and Exhibition, Vienna, Austria, June 13–17, 2004, Paper No. 2004-GT-53250. Manuscript received by IGTI, October 1, 2003; final revision, March 1, 2004. IGTI Review Chair: A. J. Strazisar.

boundary layers on each surface do not merge and, therefore, the effect of the relative wall (shroud) movement is inconsequential. This range is relevant to the assessment given that the length of the flow path along the blade tip relative to the clearance gap ranges between 2.5 near the trailing edge for the smallest gap to 25 near the leading edge (thickest part of the airfoil) for the largest gap. Lending further credibility to the hypothesis of Mayle and Metzger are the works of Chyu et al. [6] with a shroud surface moving over a simple rectangular cavity and Srinivasan and Goldstein [7] with a moving wall over a turbine blade. In particular, the work of Srinivasan and Goldstein showed only small effects of the wall motion on their measured Sherwood numbers (heat-mass transfer analogy) in the leading-edge region where the path length-to-clearance gap was larger (30) than the criterion stated by Mayle and Metzger (20) for the smallest clearance gap that they studied. For the largest gap in their study, they saw no noticeable effect of the wall motion.

The only reported tip-blowing studies were those completed by Kim and Metzger [8] and Kim et al. [9], who used a two-dimensional channel with a number of different injection geometries, and by Kwak and Han [10,11], Acharya et al. [12], and Hohlfeld et al. [13], who all used blade geometries. Four tip-blowing geometries were investigated by Kim et al. [9], which included the following: discrete slots located along the blade tip, round holes located along the blade tip, angled slots positioned along the pressure side, and round holes located within a cavity of a squealer tip. For a given coolant flow, the best cooling performance was obtained using the discrete slot configuration whereby an optimum blowing ratio was discerned. In general, Kim et al. reported higher effectiveness accompanied by higher heat transfer coefficients with higher injection rates. Kwak and Han [10,11] reported measurements for varying tip gaps with cooling holes placed along the pressure surface at a 30 deg breakout angle, relative to the pressure surface, and on the tip surface for an unshrouded [10] and shrouded [11] tip. For the unshrouded (flat) tip, Kwak and Han found that increases in the heat transfer coefficients and adiabatic effectiveness occurred with increased coolant injection and increased gap heights. This is in contrast to the work presented by Kim et al. [9], who identified an optimum blowing ratio. For the shrouded tip, Kwak and Han indicated a benefit of having a shroud in that there was a reduction of the heat transfer coefficients and an increase in adiabatic effectiveness levels when compared to the flat tip.

Heat transfer measurements on flat tips with no cooling have been presented by many authors, including Bunker et al. [14], Kwak and Han [10], and Jin and Goldstein [15]. These studies have shown there to be a region of low heat transfer located near the thickest portion of the blade. Morphis and Bindon [2] and Bindon [16] have also shown there to be a separated region followed by a reattachment with high heat transfer coefficients along the pressure side of the blade tip in the entry region [14].

Table 1 Geometry for the blade tip model

Parameter	Scaled model
Scaling factor	12×
Axial chord, B_x (% Span)	63
True chord, C (% Span)	96.3
Pitch, P (% Span)	78
Re	2.1×10^5
Inlet angle, θ	16.5 deg
Coolant to mainstream ΔT	25 deg
Small tip gap, h (% span)	0.545
Large tip gap, H (% span)	1.635

There have also been only a relatively few computational predictions for a tip gap with blowing, including those by Acharya et al. [12] and Hohlfeld et al. [13]. Acharya et al. found that film-coolant injection lowered the local pressure ratio and altered the nature of the leakage vortex. High film-cooling effectiveness and low heat transfer coefficients were predicted along the coolant trajectory. Both studies indicated that for the smallest tip gap, the coolant impinged directly on the shroud; but as the gap size increased, predictions indicated that the coolant jets were unable to impinge upon the shroud.

In summary, only one experimental study has addressed blowing in the tip gap of a turbine blade. The objectives of the work presented in this paper are to present the benefits of film-cooling of a blade tip using coolant exhausted from dirt purge holes. In particular, both the effectiveness levels and heat transfer coefficients were measured and combined using a net heat flux reduction to evaluate the benefits.

Experimental Facility and Methodology

The experiments were conducted in a large-scale, low-speed, closed-loop wind tunnel that provided matched-engine Reynolds number conditions. The flow conditions and relevant geometry are summarized in Table 1 with a diagram of the wind tunnel and test section shown in Figs. 1 and 2. Results reported in this paper include adiabatic wall temperature measurements and heat transfer coefficients along the tip.

The wind tunnel, shown in Fig. 1, includes a 50 Hp fan that drives the flow through a primary heat exchanger to obtain a uniform temperature profile. The flow is divided into three passages. The main passage, located in the center, has a heater used to achieve a hot mainstream gas, while the flow in the two outer passages provided a single row of normal jets used to generate an inlet turbulence level to the cascade of 10% and an integral length

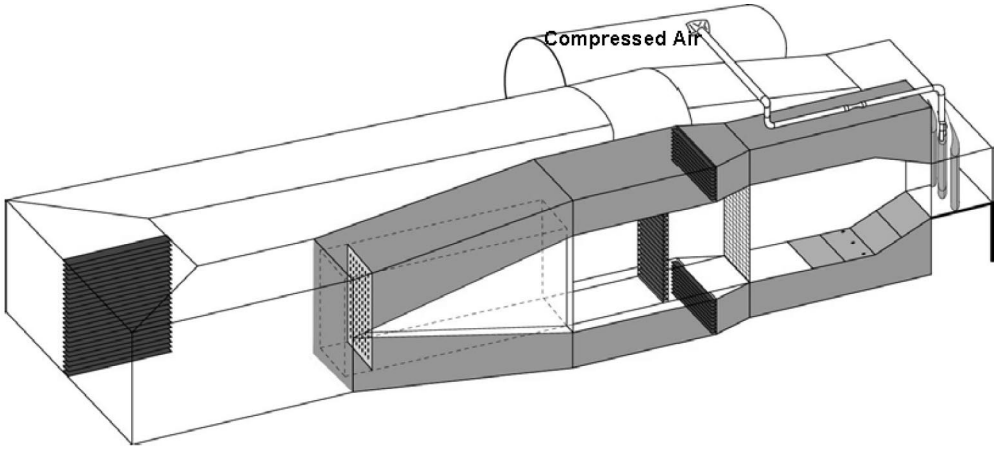

Fig. 1 Schematic of the wind tunnel facility used for the testing of the blade tips

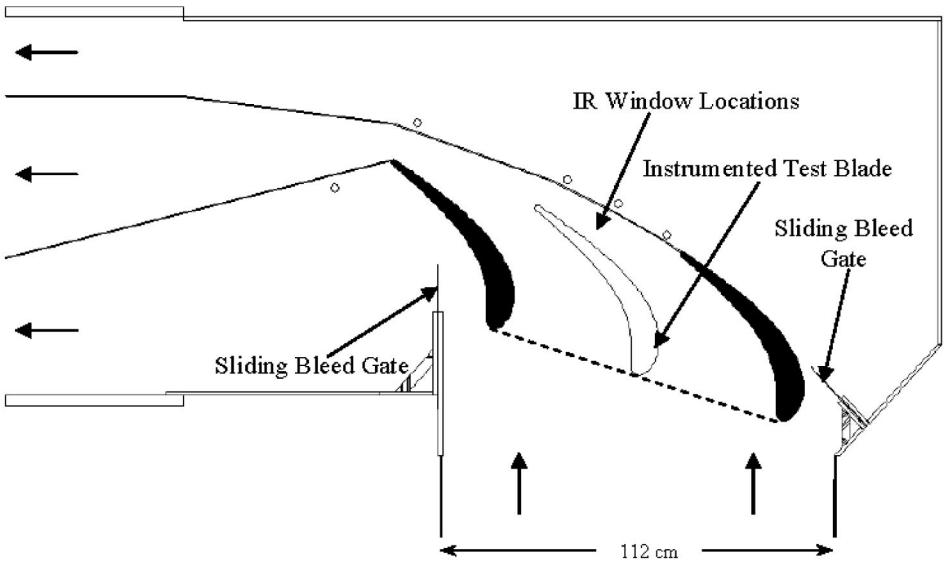

Fig. 2 The corner test section of the wind tunnel housed three blades that formed two full passages

scale of 11 cm. To quantify the integral time scale, velocity fluctuations were measured using a hot-wire anemometer. These jets were unheated (due to a facility constraint) and were injected one chord upstream of the blade. The mass flow of the injected jets represented 4.3% of the core mass flow and had a momentum flux ratio of 8. Because of the high turbulence generated, the thermal field entering the cascade was quite uniform.

The main features of the linear cascade test section, shown in Fig. 2, were an instrumented center blade, two outer blades, sidewall bleeds, and adjustable tailboards. These components were required to ensure periodic flow conditions. Coolant flow for the blade tip was provided to a plenum inside the center blade from an independent pressurized air supply. The pressure drop across a venturi meter was used to quantify the coolant flow rate, while the incoming velocity to the test section was measured with a pitot probe at several locations across the blade pitch.

Figure 3 shows the details of the plenum for the blade tip, the dirt purge cavity, and the dirt purge holes. The removable portion of the tip was 28% of the span (total span was 55 cm) and was specifically molded to allow for a number of different tip geometries to be studied. A two-part foam mixture that exothermically expanded was used to mold the blade tip. The thermal conductivity of this foam was quite low at 0.036–0.043 W/mK and was dependent on the foam properties after expansion, thereby allowing for an adiabatic surface on the blade tip. Only the foam surface (no heater) was present during the adiabatic effectiveness tests.

For the adiabatic effectiveness tests, the experiments were conducted such that the coolant was nominally 25°C lower than the mainstream. Thermal equilibrium required about 4 hr for each test. For the heat transfer measurements, separate experiments were performed with a constant heat flux surface installed on the tip surface. For these tests, the coolant and mainstream temperatures were typically kept to within 0.15°C of one another. Two separate heaters were necessary because of the dirt purge cavity on the tip. The dirt purge cavity was heated with one strip of Inconel that was 0.051 mm thick and had a surface area of 17.3 cm^2. The main heater covered an area of 261.2 cm^2 and consisted of a serpentine Inconel circuit. As shown in Fig. 4, the circuit consisted of the Inconel sandwiched between insulating Kapton and then covered with a very thin (0.013 mm) layer of copper on both sides. Both heaters were attached to a foam blade tip using double-sided tape that was 0.64 mm thick. The nominal heat flux for both heaters was set to 3700 W/m^2, which provided a maximum temperature difference between the mainstream and blade surface of 28°C. The two heaters were controlled independently to within 0.67% of one another during all tests. The current supplied to each heater was known by placing a precision resistor ($R = 1.0\Omega \pm 0.1\%$) in each circuit and measuring the voltage drop across each resistor with a digital multimeter. The heater power was then determined from the supplied current and known heater resistance.

Equation (1) was used when calculating the heat transfer coefficients,

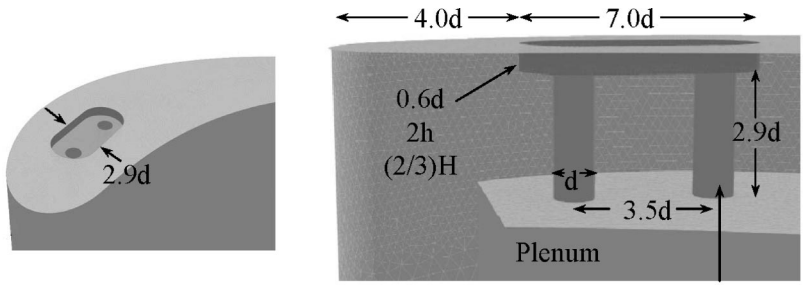

Fig. 3 The blade tip included a plenum that supplied coolant to the dirt purge holes

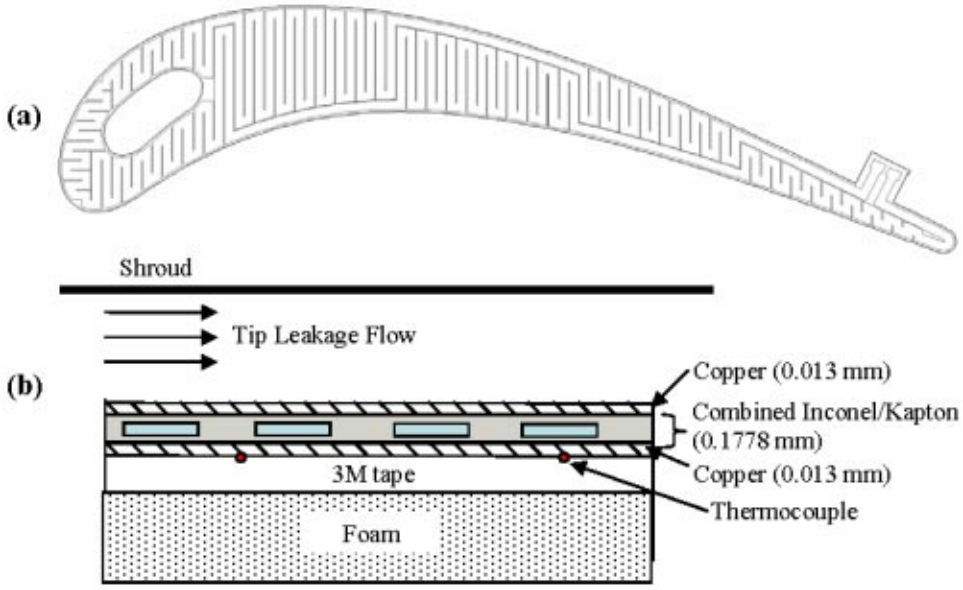

Fig. 4 Main tip heat transfer surface showing (*a*) serpentine passages and (*b*) detail of main tip heater as placed on the blade surface

$$h=(q''_{\text{tot}}-q''_r)/(T_w-T_\infty) \quad (1)$$

In this equation, q''_{tot} represents the total heat flux output from the resistive heaters and q''_r represents the energy lost to radiation. Typically, radiation losses were less than 2% with the maximum for all cases being 3.4%. Conduction losses were found to be negligible because the heaters were placed on the low-thermal conductivity foam.

For the surface-temperature measurements along the tip, an infrared (IR) camera was used to take four separate images that were then assembled to provide the entire surface temperatures of the tip. The image locations are shown by the boxes in Fig. 2. The IR camera was positioned to look directly at the blade tip and required the use of a zinc selenide window placed along the outer shroud that permitted 8–12 micron wavelengths to pass through. Each of the four IR camera images covered an area that was 21.3 cm by 16 cm with the area being divided into 320 by 240 pixel locations. The camera was located approximately 55 cm from the tip, resulting in a spatial resolution of 0.63 mm, which is over 16 times smaller than the dirt purge hole diameter. At each viewing location five images were acquired and averaged at each pixel location to give an overall image of the tip.

The calibration process for the camera involved direct comparisons of the infrared radiation collected by the camera with measured surface temperatures, using either thermocouple strips placed on the tip surface (for the adiabatic effectiveness measurements) or thermocouple beads placed underneath the heater (for the heat transfer measurements). For both experiments, thermocouples were placed on the blade surface using a bonding agent with a high thermal conductivity of 1.6 W/mK. For the thermocouples placed underneath the main tip heater, a 2°C temperature adjustment was applied during calibration to account for the thermal resistivity of the heater at the nominal $q''=3700\,\text{W/m}^2$. The thermal resistance of the Inconel heater in the dirt purge cavity was found to be negligible, and no correction was needed for this area of the blade tip. After the experiments were completed, the infrared images were processed, where adjustments of the surface emissivity and background temperature (irradiation) were made until the image and thermocouple temperatures matched. This process resulted in an agreement between all of the thermocouples and infrared temperatures to within ± 1.0°C ($\Delta\eta=\pm 0.04$). A check on the calibration process is that the four individual images matched up well to form one entire blade contour without any discontinuities in measured values between images.

Static-pressure taps were located near the midspan of the central blade, and tufts were located near the stagnation locations of all the blades to ensure periodic flow through the passages was achieved. The measured static-pressure distribution around the center blade was compared with an inviscid CFD simulation using periodic boundary conditions, as shown in Fig. 5. This pressure loading is representative of a modern, high-pressure turbine blade.

Overall uncertainties were calculated for nondimensional temperature and heat transfer (η and Nu values) according to the partial derivative method described in Moffat [17]. The total uncertainty of all measurements was calculated as the root of the sum of the squares of the precision uncertainty and the bias uncertainty.

The precision uncertainty for measurements made with the in-

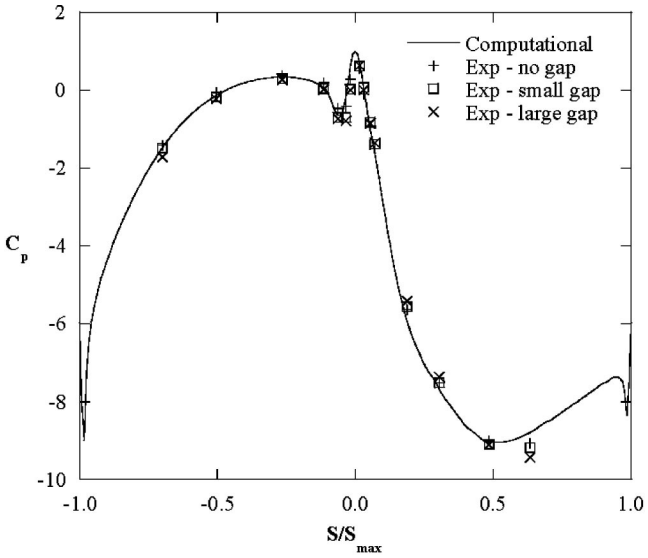

Fig. 5 Measured and predicted static pressures at the blade midspan

Table 2 Matrix of experiments and blowing ratios

Coolant flow (% total flow)	Tip gap	Holes 1 and 2		Hole 1		Hole 2	
		Global M	Global I	Local M	Local I	Local M	Local I
0.10	small, large	1.4	3.6	1.9	6.6	1.1	2.1
0.19	small, large	2.7	13.0	3.6	23.7	2.0	7.5
0.29	small, large	4.1	30.3	5.5	55.3	3.1	17.4
0.38	small, large	5.3	52.0	7.2	94.9	4.1	29.9

frared camera was determined through an analysis of five calibrated images taken in succession on one portion of the tip at constant conditions. The precision uncertainty was calculated to be 0.31°C, which is the standard deviation of the five readings based on a 95% confidence interval. The camera manufacturer reported the bias uncertainty as 2.0% of the full scale. The largest scale used in this study was 20°C though some images could be captured on a 10°C range. A bias error of ±1°C was considered for the camera calibration. The thermocouples measuring the freestream and coolant temperatures were reported by the manufacturer to read within ±0.2°C. The total uncertainty in effectiveness was found to be $\delta\eta=\pm 0.046$ at $\eta=1$ and $\delta\eta=\pm 0.046$ at $\eta=0.2$. The total uncertainty in heat transfer measurements was 6% at $\mathrm{Nu}_{Dh}=45$ and 10.5% at $\mathrm{Nu}_{Dh}=55.7$. Note that the uncertainty is higher in the immediate vicinity of the dirt purge holes where the heat flux is not uniform. The nonuniformity of the heat flux does not affect the ratios of the heat transfer coefficients with and without blowing, however, because this effect is canceled.

Experimental Test Cases

This series of experiments focused on investigating the effect of tip gap height and blowing ratio as indicated in Table 2. With regard to the tip gap height, two different gaps relative to the span were investigated, including gaps that were 0.54% (h) and 1.63% (H) of the span. Through the remainder of this paper these two tip gaps will be referred to as small and large tip gaps. With regard to the blowing from the dirt purge holes, cases at each tip gap height were measured with a coolant flow rate that ranged from 0.10% to 0.38% of the primary core flow. Note that these flow rate ranges were chosen to simulate engine conditions. A baseline case was also considered for heat transfer measurements that had the dirt purge cavity present, but no holes. Measurements were performed at both gap heights for the baseline case.

The global and local ratios of mass and momentum fluxes were calculated for the blowing cases and are also given in Table 2. The global mass and momentum flux ratios were based on the incident inlet velocity to the blade passage, while the local mass and momentum flux ratios were based on the local tip flow conditions for each of the two dirt purge holes. To compute the local external velocity for the dirt purge hole exits, the local static pressure for the dirt purge holes was taken as the average of the predicted static pressures for the pressure and suction surfaces at the 95% blade span location. The blade locations of these pressures were at 2% and 5% of the total surface distance measured from the stagnation location for dirt purge holes 1 and 2, respectively. The coolant velocity was calculated directly from measured coolant flow rates. As seen in Table 2, the local blowing (and momentum) ratio for hole 1, which is the hole closest to the leading edge, is significantly higher than hole 2 due to the lower local velocity present at the hole 1 location.

Adiabatic Effectiveness Results

The dirt purge holes serve the functional purpose of expelling dirt from the blade that might otherwise block smaller film-cooling holes. Any cooling from the dirt purge holes is of potential benefit for cooling the leading-edge region. The cooling effects of the dirt purge jets are presented as adiabatic effectiveness levels that were measured only in the leading-edge half of the blade. No coolant from the dirt purge holes was measured along the downstream portion of the blade tip, and as such, only the front portions of the tip were measured.

Figure 6 presents the measured adiabatic effectiveness contours for the small tip gap case at four different blowing ratios, ranging from 0.10% to 0.38% (percents based on passage flow). At the lowest blowing ratio, the dirt purge holes cool only a portion of the tip downstream of the holes. There is very little cooling measured within the dirt purge cavity. There is a dramatic increase in the measured adiabatic effectiveness levels as the coolant flow is increased for the small tip gap. The maximum effectiveness for the lowest blowing ratio was 0.86 while a maximum value of $\eta=1.0$ was reached for the 0.19%, 0.29%, and 0.38% blowing ratios. For coolant injection greater than the 0.19% case, a completely cooled region was measured to extend from the pressure side of the tip to the suction side. Interestingly, the coolant is also present upstream of the dirt purge holes such that at the highest blowing ratio, the coolant extended to the leading edge of the tip. This is because the coolant exiting the dirt purge holes impacted the shroud and then propagated outward in all directions. These very high effectiveness levels in the leading-edge region indicate a saturation of the coolant within the tip gap. In general, this is consistent with field-run hardware where this portion of the airfoil has little evidence of tip oxidation.

Figure 7 presents the measurements of adiabatic effectiveness contours for the large tip gap. Results indicate a significantly reduced benefit of the coolant exiting the dirt purge holes as compared to the small tip gap. As the coolant is increased, the experiments show a much broader cool region downstream of the cavity. This spreading of the coolant for the higher blowing ratio cases is caused by an impingement of the jets onto the shroud. At the

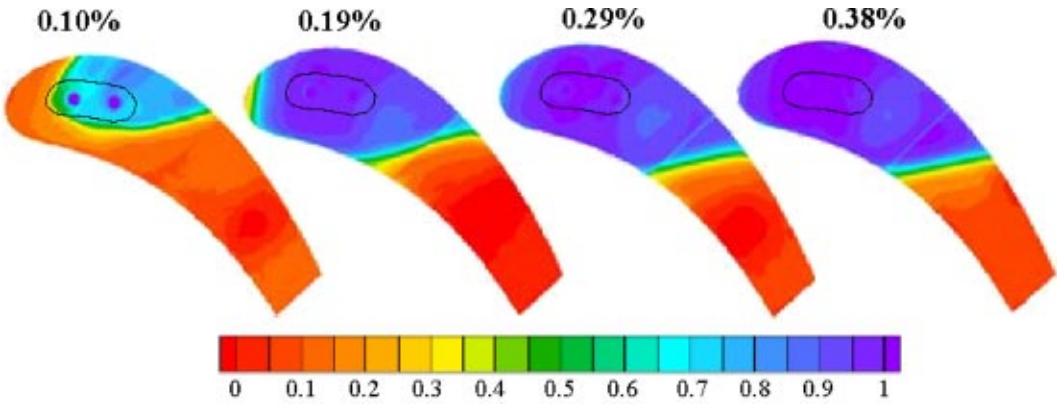

Fig. 6 Adiabatic effectiveness contours taken along the tip with dirt purge blowing for the small tip gap

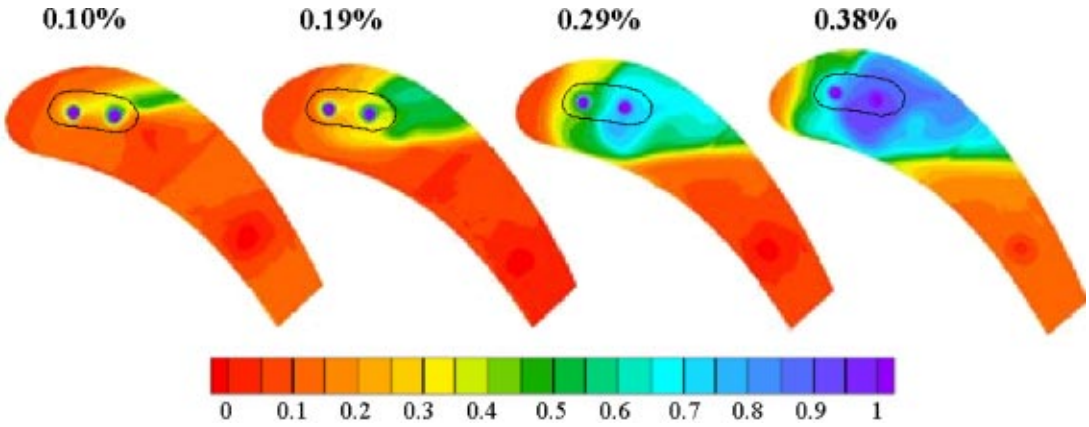

Fig. 7 Adiabatic effectiveness contours taken along the tip with dirt purge blowing for the large tip gap

0.38% coolant injection, there is coolant present with the dirt purge cavity and upstream of the cavity. This is more similar to the small tip gap where coolant is filling the entire gap.

The camber line of the blade is used to compare data and is defined in Fig. 8. This line extends through the midsection of the blade. Effectiveness data were taken along the camber line of the blade, shown in Fig. 9, to further illustrate the differences between the cases tested. The vertical lines on both plots indicate the location of the dirt purge holes. For the small tip gap shown in Fig. 9(*a*) the 0.10% case has significantly lower effectiveness values than the other coolant levels. For the 0.19%, 0.29%, and 0.38% cases, there is hardly any difference in peak values between the cases, but there is increased spreading in the leading-edge region with increased blowing. Also, at the higher blowing ratios, the camber line shows that the adiabatic effectiveness reaches a value of one almost all the way to the stagnation point ($x/C=0$). For the large tip gap shown in Fig. 9(*b*) the effectiveness steadily increases with each blowing case, as was discussed for the contour levels. Both the peak values and spreading in the leading edge are increased with each increase in blowing rate. However, there appears to be no benefit of nearly doubling the coolant flow from 0.10% to 0.19% at the large tip gap until downstream of the second hole after which there is more spreading of the coolant for the higher coolant flow. Also, the overall effectiveness levels are lower at the large tip gap relative to the small tip gap.

For all cases shown in Figs. 9(*a*) and 9(*b*), the results indicate η values that are above zero outside of the region affected by the dirt purge blowing. The reason for this nonzero effectiveness level is due to a thermal boundary layer effect. As was discussed in the experimental section of this paper, the heaters for the main gas path are located significantly upstream of the test section. As the flow progresses through the contraction of just upstream of the test section, the flow near the wall is slightly cooler than the midspan temperature, resulting in nonzero effectiveness levels.

All of the adiabatic effectiveness measurements for dirt purge cases are summarized by considering an area average that was calculated for a region defined from the leading edge to a location along the pressure side of $s/C=0.3$. A line drawn normal to the pressure side extending to the suction side defines the area. These area averages, which represent effectiveness averages over 46% of the total blade tip area, are shown in Fig. 10. Overall there is a dramatic difference between the small tip gap and the large tip gap at each blowing ratio. The small tip gap shows the average effectiveness increases with blowing ratio, but is leveling off at the higher injection levels. The area averages for the large tip gap case show that the effectiveness only slightly increases when the blowing ratio is increased from 0.10% to 0.19% with larger increases being measured beyond 0.19% injection levels.

Heat Transfer Results

As discussed, separate experiments were performed to measure heat transfer for baseline cases with no blowing and for the blowing cases at both tip gap heights. These measurements were completed using a constant heat flux boundary condition on the tip surface. Baseline studies with no blowing were used to validate the current experiments with previous ones by comparing with a fully developed channel flow correlation. The heat transfer for the blowing cases was normalized by the baseline cases to provide the heat transfer augmentation associated with each blowing case considered. Also, the results from the adiabatic effectiveness experiments were combined with these heat transfer measurements to quantify the overall blade thermal loading for each of the blowing cases.

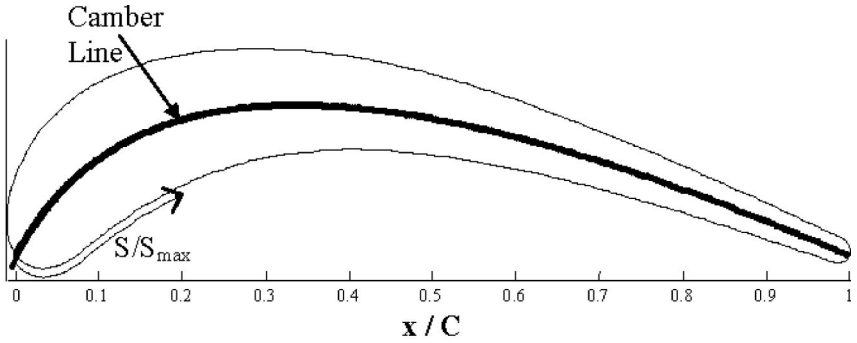

Fig. 8 Definition of the blade camber line

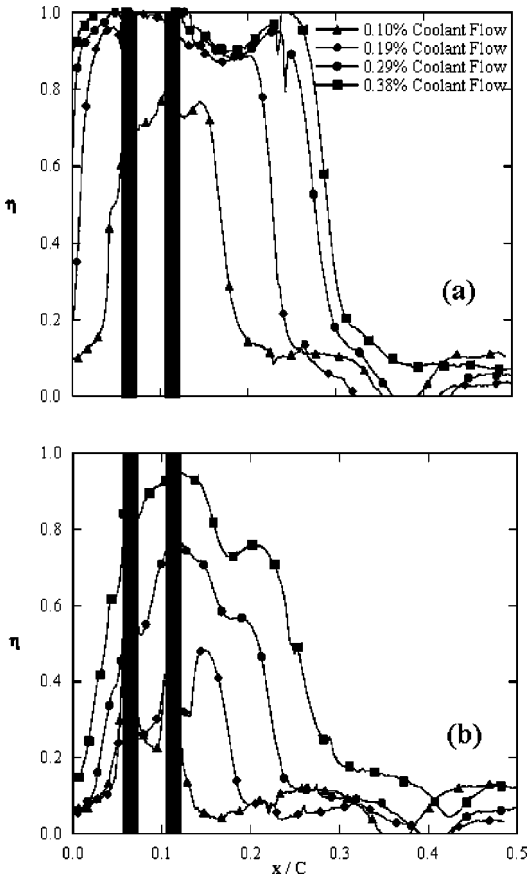

Fig. 9 Effectiveness taken along the blade camber line for the (*a*) small and (*b*) large tip gaps

Baseline Cases—No Blowing. Previous studies have compared flow in a turbine blade tip gap to that of a fully developed channel flow correlation for turbulent flow in a duct. The correlation that was used for comparison was developed by Gnielinski [18]. Gnielinski's correlation is given in Eq. (2) and has been reported in the literature to provide accuracy to within 6% as reported by Kakaç et al. [19] for a large Reynolds number range ($10^4 < \mathrm{Re} < 10^6$).

$$\mathrm{Nu}_{fd} = 0.0214(\mathrm{Re}^{0.8} - 100)\mathrm{Pr}^{0.4} \tag{2}$$

Mayle and Metzger [5] furthered this correlation for a tip gap by adding an augmentation factor to account for the overwhelming entry-region effects of thin blade tips. This augmentation factor, which was taken from Kays and Crawford [20], allows blade designers to relate overall blade tip heat transfer (for a given blade thickness and tip gap) to an overall heat transfer expected in a fully developed channel as shown in Eq. (3). Equation (3), as pointed out by Mayle and Metzger [5], accounts for the fact that only one side of the channel (blade tip) was heated.

$$\mathrm{Nu}/\mathrm{Nu}_{fd} = 1 + \frac{3}{L_t/D_h} \tag{3}$$

Comparisons have been made to the data of Jin and Goldstein [15] and Bunker et al. [14] that confirm this augmentation factor approach. Although Mayle and Metzger [5] first noted the augmentation factor, their data have not been included in this comparison because only experiments performed on airfoil shapes were considered. This is because the plotting variables were based on blade exit velocity, of which there is no equivalent in the Mayle and Metzger tests. Figure 11 shows Nusselt number values based on the hydraulic diameter of the tip gap (2h or 2H) plotted as a function of the blade Reynolds number based on the exit velocity and hydraulic diameter. The Gnielinski correlation has been plotted for several L_T/D_h ratios as shown on the plot. Note that L_T represents the maximum thickness of the blade. As known for turbulent channel flow, fully developed conditions generally occur for $L/D_h > 20$ [20]. The correlations given in Fig. 11 indicate similar trends to the experimental data despite very different blade shapes with the largest outliers occurring at the lowest blade Reynolds numbers (not tip gap Reynolds number). It should be noted that the L_T/D_h ratios are based on the maximum blade thickness, and the Nusselt numbers are the average values calculated for the tip surface. Therefore, this ratio is not a perfect representation of a blade profile. More experiments should be performed to further verify this trend.

The baseline results are presented as contour plots of Nusselt number (based on chord) in Fig. 12. Note that the chord rather than hydraulic diameter was used for these contour plots to illustrate the differences in the heat transfer coefficients along the blade tip for both tip gaps. Also, it is important to recognize that the heat flux is not uniform in the immediate vicinity of the dirt purge holes. Results at both gap heights show similar trends, however, the large tip gap shows higher Nusselt numbers at the blade trailing edge relative to the small tip gap. This increase in heat transfer at the larger tip gap trailing edge is a result of the increased entry region effect relative to the small tip gap. With smaller L/D_h values (for the large tip gap), the entry region is expected to have a greater effect, as mentioned at the beginning of this section. For the large tip gap, the L/D_h is as low as 1 across the trailing edge of the tip surface, whereas for the small tip gap the L/D_h is 3.5.

The area-averaged Nusselt numbers are given for each case to quantify the increase in heat transfer with gap height. For these cases, the Nusselt number at the large tip gap is 3.2 times that of the small tip gap when based on the exit velocity and hydraulic diameter. By using Reynolds number scaling for a turbulent channel flow, the large tip gap is expected to have 2.4 times the heat transfer of the small tip gap. This larger than expected increase results from the overwhelming entry region effects, which serve to greatly increase the tip heat transfer.

As shown in Fig. 12, there are regions of low heat transfer immediately downstream of the dirt purge cavity for both tip gap heights. This is near the thickest portion of the blade and represents the area of lowest heat transfer on the blade tip. This region

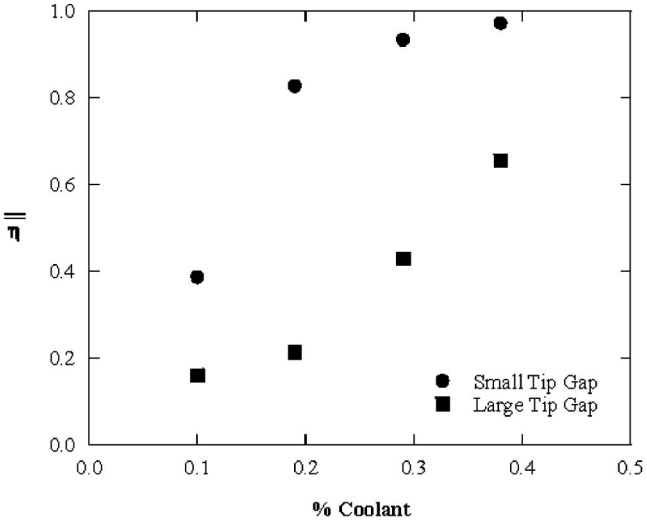

Fig. 10 Area-averaged effectiveness of the tip at various coolant blowing levels

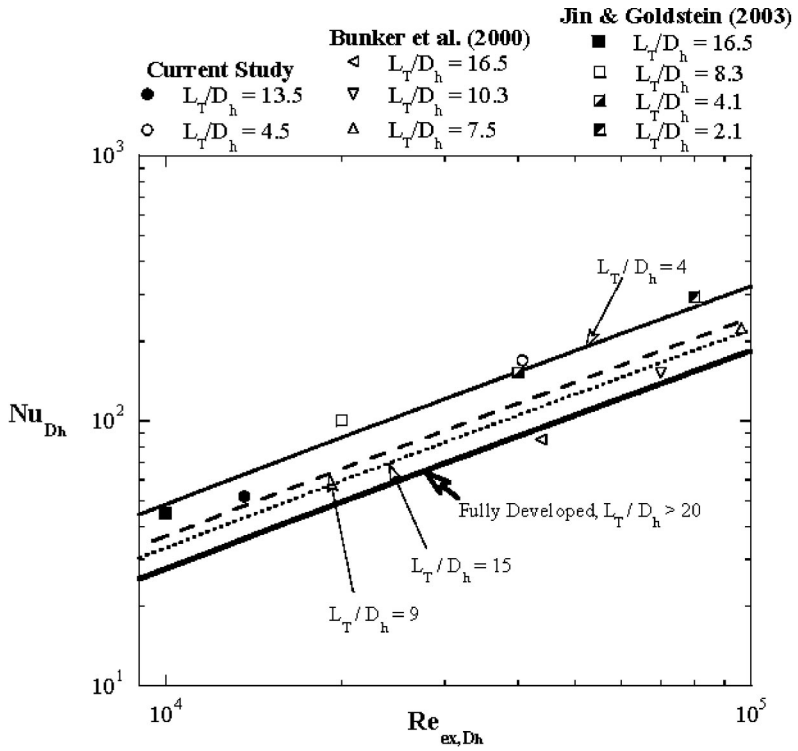

Fig. 11 Comparison of experimental data to a fully developed correlation

was first pointed out by Bunker et al. [14] and has been confirmed by other authors. Within the dirt purge cavity, there are high heat transfer coefficients resulting from low velocity flow recirculation in the cavity. Overall, the leading-edge region experiences relatively low heat transfer outside of the dirt purge cavity relative to the trailing edge.

Also seen on these contour plots are regions of high heat transfer along the pressure side that begin around $S/S_{max}=0.1$ and extend until the trailing edge. These regions of high heat transfer have been noted by Morphis and Bindon [2] and Bindon [16] to be the separation-reattachment region that forms along the pressure side due to mainstream and leakage flow interaction. This region occurs within the entry region, is more dominant at the large tip gap than at the small tip gap, and extends over a large region of the tip for the large tip gap.

Heat Transfer Augmentation With Blowing. By comparing the heat transfer with blowing to that of the baseline cases, the augmentation associated with tip blowing can be studied. The camber line plots for the dirt purge blowing are shown in Figs. 13(*a*) and 13(*b*) for the small and large tip gaps, respectively. For both tip gaps, the heat transfer is increased with blowing for the

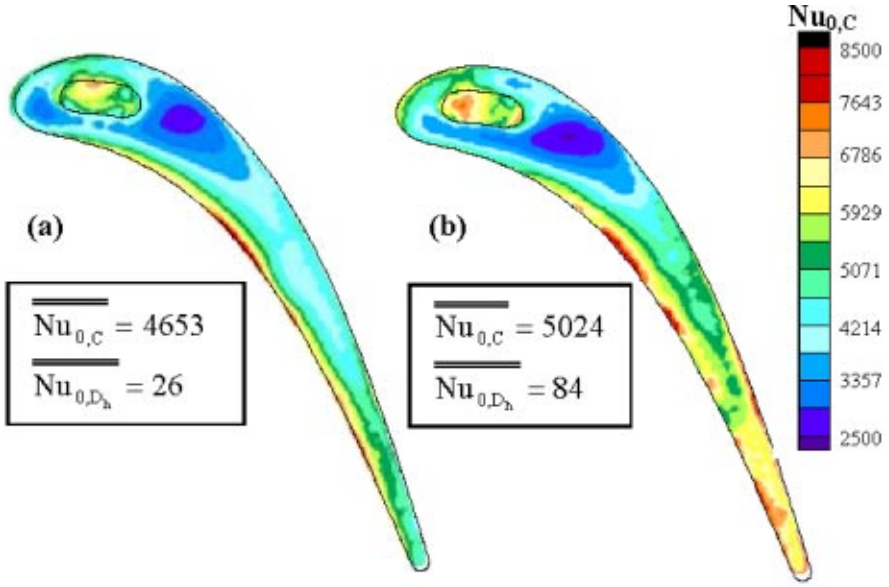

Fig. 12 Baseline Nusselt number contour plots for the (*a*) small and (*b*) large tip gap heights

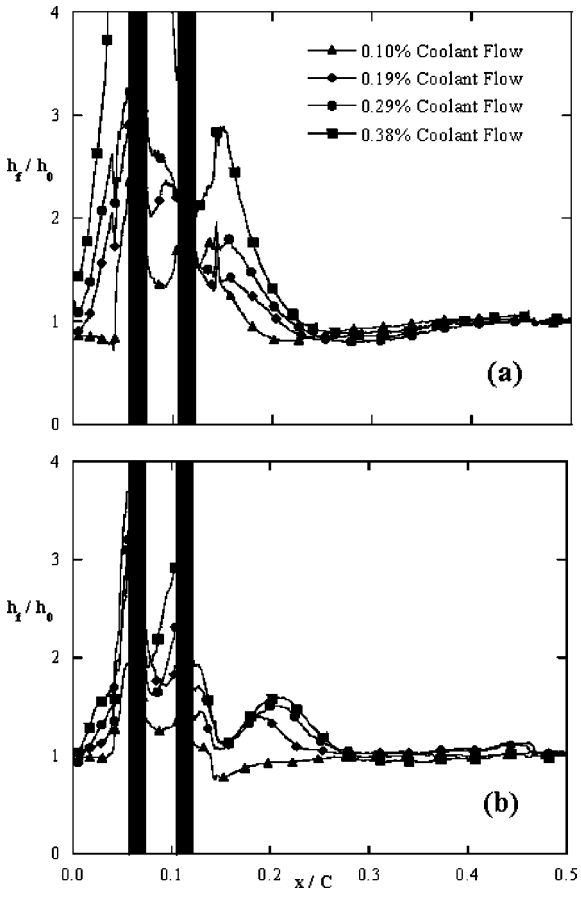

Fig. 13 Camber line data for h_f/h_0 for the (*a*) small and (*b*) large tip gaps

region of $0<x/C<0.25$. Beyond $x/C=0.3$, there is no difference between any of the cases because the dirt purge blowing does not affect heat transfer in this area. In comparing Fig. 13 with Fig. 9, there are striking differences between the two data sets. The film-cooling effectiveness (Fig. 9) extends further down the blade than does the heat transfer augmentation. For the small tip gap, the film cooling remains near $\eta=1$ out to $x/C=0.25$ for the highest blowing ratio, whereas the heat transfer augmentation is at a value of one at that location. This shows that for the small tip gap, the dirt purge holes are impinging upon the shroud and effectively spreading coolant flow while the heat transfer increase is localized around the hole exits. For the large tip gap, there are localized peaks of film effectiveness for each of the three highest blowing ratios located at $x/C=0.15$ for the 0.19% case, and near $x/C=0.2$ for the 0.29% and 0.38% cases. These peaks of adiabatic effectiveness correspond to peaks of heat transfer. At the 0.29% and 0.38% cases, the peaks are located at the same position, suggesting that the coolant flow has impinged upon the shroud and returned back to the tip. For the 0.19% case, however, the peaks are not colocated. Instead, the peak in heat transfer is located downstream of the peak in film effectiveness. This suggests that at this particular blowing ratio, the dirt purge jet is causing flow vortices to form near the jet that do not cause high film effectiveness, but do increase the heat transfer.

CFD results by Hohlfeld [21] predicted these voritices. Coolant-flow streamlines for the large tip gap are shown in Fig. 14. At the highest blowing ratio (0.38%), the coolant is spread in all directions after hitting the shroud. At the 0.19% case, the first dirt purge hole is split by the second hole such that part of the flow rolls into a vortex around the right side of the second hole jet. This vortex extends the full gap height and is what causes the

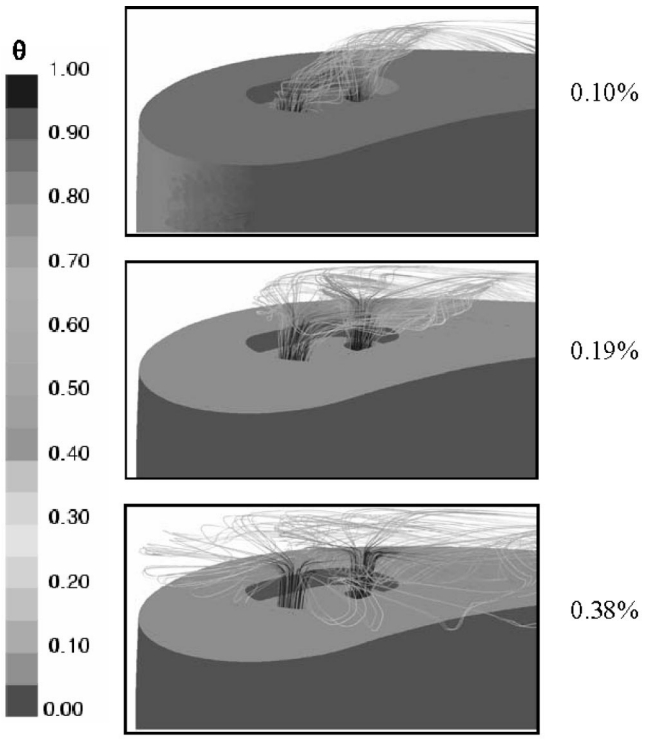

Fig. 14 CFD predictions of dirt purge streamlines for the large tip gap [21]

peak in heat transfer to be located further downstream than the peak in film effectiveness for this case. The 0.10% case is shown to verify that there are no vortices at this case, but rather flow exiting the holes and immediately flowing out of the gap region.

Peaks of heat transfer are seen immediately around both of the dirt purge holes in Fig. 13. The reason for this is that the holes cut out of the foil heater had high current gradients very near to the holes, resulting in high heat transfer coefficients.

Area averages of the heat transfer augmentation for both tip gaps are shown in Fig. 15. Again, these averages are over the forward 46% of the blade tip area, so that only the area affected by the blowing is considered. These results show there to be the same heat transfer augmentation for the lowest blowing ratios at

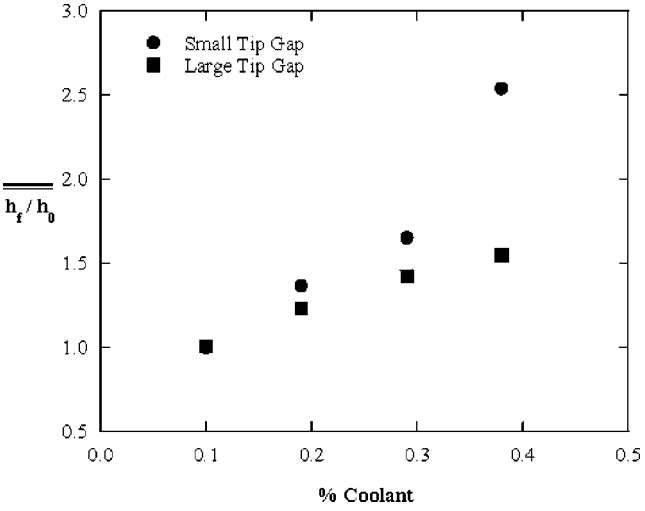

Fig. 15 Area-averaged heat transfer augmentation for the small and large tip gaps

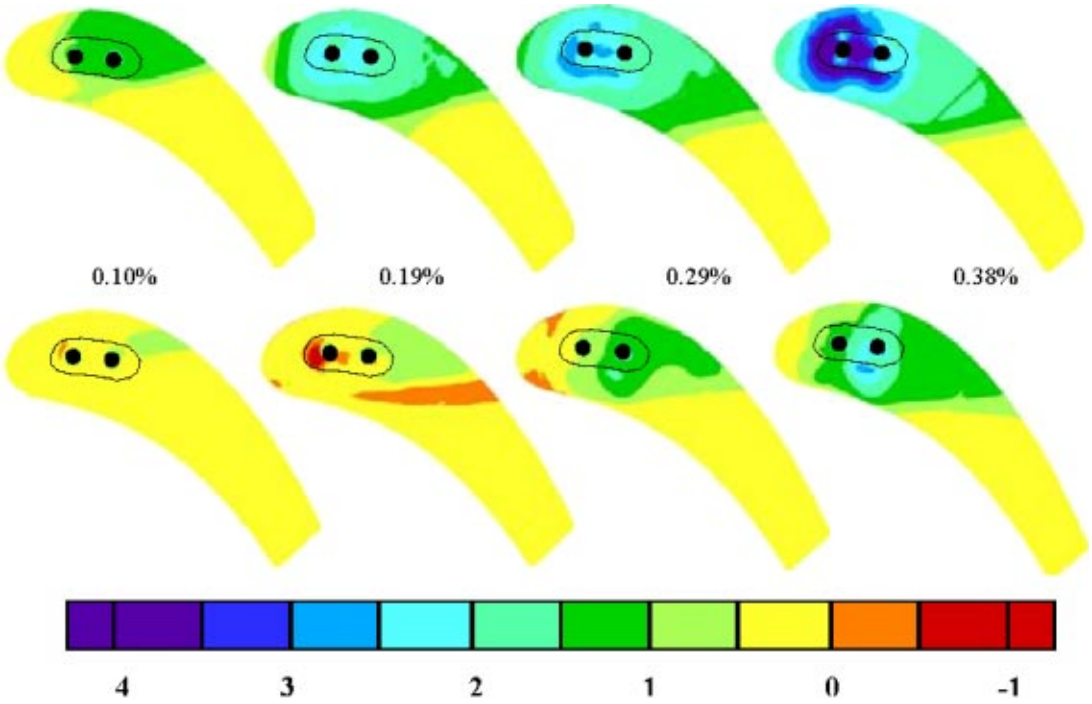

Fig. 16 Contour plots of NHFR for the small (top) and large (bottom) gap heights at all blowing ratios

both tip gaps. As the blowing ratio increases, however, the small tip gap shows increasingly higher augmentation than the large tip gap. This higher augmentation is because of the influence of the three-dimensional vortices formed as the jets exit the dirt purge holes. As was discussed in the adiabatic results section, flow from the dirt purge holes for the small tip gap can flood the leading-edge gap region, causing very good cooling over most of the leading edge. At the large tip gap, the flow is blowing off the tip surface and impinging on the shroud. Because of this, the augmentation is higher at the small tip gap than at the large tip gap for the same blowing ratio.

Net Heat Flux Reduction. Combining the heat transfer measurements with the film effectiveness measurements can give the overall cooling benefit in the form of a net heat flux reduction (NHFR). Shown in Eq. (4), NHFR is an established method of evaluating the overall effect of a cooling scheme on a surface [22],

$$\mathrm{NHFR} = 1 - (h_f/h_0)[1 - \eta \cdot \theta)] \tag{4}$$

All variables have been measured experimentally except for θ, which was assumed to be 1.6 based on previous literature [22]. This value corresponds to a cooling effectiveness of 62.5%. As this equation shows, when high heat transfer augmentation is not accompanied by high film cooling, the NHFR can become negative. A negative NHFR means that there is an increased heat load to the blade surface, which is undesirable.

The NHFR values were calculated locally for each case and are shown in Fig. 16. The NHFR is always higher at the small tip gap relative to the large tip gap. This can be attributed to the much higher film-cooling effectiveness and only slightly higher heat transfer augmentation of the small tip gap relative to the large tip gap. At the small tip gap, the NHFR always increases with blowing. For the large tip gap, the area downstream of the dirt purge cavity shows increased NHFR values with increased blowing, however, for the entire leading-edge region, the 0.19% case appears to be lower than the 0.10% case. This is because of the slightly negative NHFR downstream of the second dirt purge hole. This region is caused by the vortices created by the dirt purge blowing, which are not seen in any of the other cases, as was previously discussed.

NHFR values along the camber line are shown in Fig. 17 for the small and large tip gaps. For the small tip gap [Fig. 17(*a*)], there is increased spreading of the NHFR in the region $0 < x/C < 0.3$ as blowing increases. The highest blowing case (0.38%) shows a large spike at the first dirt purge hole. This is caused by high heat transfer immediately surrounding the dirt purge hole, where the uncertainly is higher due to nonuniform heat flux, as discussed previously. For the large tip gap, there is generally increased NHFR with increased blowing with the exception of the region around $x/C = 0.2$. Around this area, the 0.19% case actually shows lower NHFR than the 0.10% case due to the decreased film effectiveness.

Area averages of the NHFR values were calculated for the forward part of the blade. The results, shown in Fig. 18, indicate the NHFR is always higher for the small tip gap. For the small tip gap, the NHFR levels increase nearly linearly with blowing ratio. For the large tip gap, however, the lowest blowing ratio shows higher NHFR values than the 0.19% case, although increases in blowing ratio result in increased NHFR.

Conclusions

Intended to prevent dirt and dust particles from clogging smaller film-cooling holes, dirt purge holes can provide significant cooling to the leading edge of a blade tip. Note that in an engine design, the entry corner and trailing-edge regions also need to be cooled. The dirt purge jets provided a significant amount of cooling for the leading-edge area, particularly for the small tip gap. From the contours and profiles on the tip for the small gap case, it was apparent that there was an overcooling of the leading-edge area for coolant injections that were greater than 0.19% of the main passage flow. Increased blowing resulted in a larger cooling benefit for the large tip gap as compared to the small tip gap, although the small tip gap always showed higher overall effectiveness for the same blowing ratio. For the large tip gap, which is most likely to occur for operating engine conditions, the lower

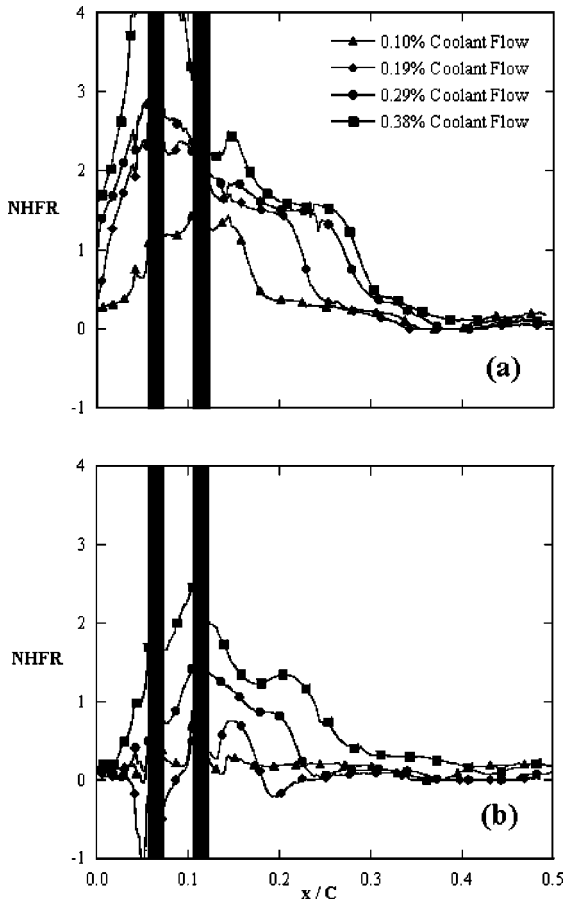

Fig. 17 NHFR taken along the Camber line for the (*a*) small and (*b*) large gap heights

coolant injection rates of 0.10% and 0.19% of the passage flow, the coolant was only effective within the dirt purge cavity and just downstream of the cavity. As the coolant injection was increased to 0.29% and 0.38% for the large tip gap, cooling was evident within, upstream, and downstream of the purge cavity.

Heat transfer measurements indicate that heat transfer augmentation with blowing is increased with higher blowing ratios for both gap heights tested. Also, the augmentation seen for the small tip gap tends to be higher than that of the large tip gap. By combining the adiabatic effectiveness and heat transfer measurements, the large tip gap experienced less benefit than the small tip gap of the dirt purge cooling. For the large tip gap, the NHFR decreased from the 0.10% case to the 0.19% case, but increased with subsequent blowing ratios. Overall, the measurements indicate that better NHFR from the dirt purge holes can be achieved for a small tip gap as compared to a large tip gap.

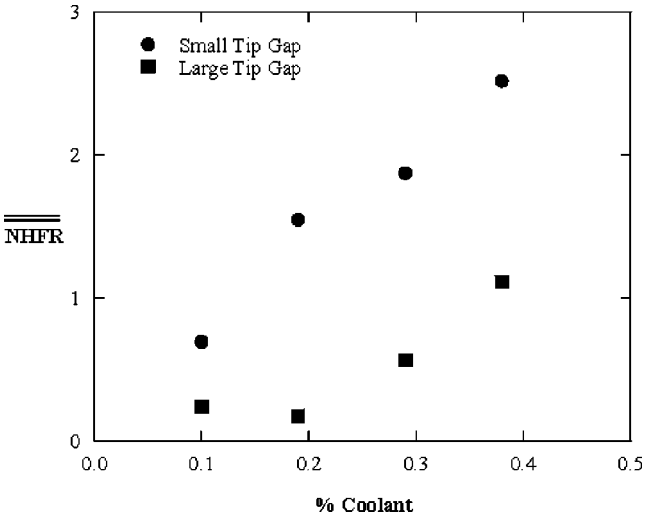

Fig. 18 Area-averaged NHFR for both gap heights

Acknowledgment

The authors gratefully acknowledge United Technologies—Pratt and Whitney for its support of this work.

Nomenclature

B_x = axial chord
C = true chord of blade
C_p = pressure coefficient, $C_p=(p-p_{in})/(\rho U_{in}^2/2)$
d = hole diameter of the dirt purge
D_h = hydraulic diameter, always used as 2h or 2H
h = small tip gap height
H = large tip gap height
h_f = film heat transfer coefficient
h_0 = blade heat transfer coefficient with no blowing
k = thermal conductivity
I = local $(\rho_c U_c^2/\rho_\infty U_\infty^2)$ or global $(\rho_c U_c^2/\rho_{in} U_{in}^2)$ momentum flux ratio
L = local thickness of blade
$L_{\max}$ = max local thickness of blade
L_T = max thickness of blade overall
$\dot{m}$ = mass flowrate
M = local $(\rho_c U_c/\rho_\infty U_\infty)$ or global $(\rho_c U_c/\rho_{in} U_{in})$ mass flux ratio
NHFR = net heat flux reduction, see Eq. (4)
Nu_{Dh} = Nusselt number based on hydraulic diameter, $h(D_h)/k$
Nu_{fd} = Nusselt number at fully developed condition based on hydraulic diameter, $h(D_h)/k$, see Eq. 2
$\mathrm{Nu}_{0,C}$ = baseline Nusselt number based on chord, $h(C)/K$
$\mathrm{Nu}_{0,Dh}$ = baseline Nusselt number based on hydraulic diameter, $h(D_h)/k$
P = blade pitch
P_o, p = total and static pressures
Pr = Prandtl number
q''_{tot} = heat flux supplied to tip surface heater
q''_r = heat flux loss due to radiation
R = resistance in Ω.
Re_{in} = inlet Reynolds number, $U_{in}(C)/\nu$
Re_{Dh} = Reynolds number based on local velocity and hydraulic diameter, $U_{local}(D_h)/\nu$
$\mathrm{Re}_{ex,Dh}$ = Reynolds number based on exit velocity and hydraulic diameter, $U_{ex}(D_h)/\nu$
Re = Reynolds number
S = surface distance along blade
T = temperature
U_{local} = local velocity on tip gap
U_{ex} = exit velocity (at blade trailing edge)
U_{in} = inlet velocity (1 chord upstream)
x = distance along blade chord

Greek

η = adiabatic effectiveness, $\eta=(T_{in}-T_{aw})/(T_{in}-T_c)$
Δ = denotes a difference in value
ρ = density
ν = kinematic viscosity
ε = emissivity of tip heater surface, always set to 0.93.
θ = dimensionless temperature ration, $(T_\infty-T_c)/(T_\infty-T_w)$, always set to 1.6.
θ_1 = dimensionless thermal field, $(T_\infty-T)/(T_\infty-T_c)$

Subscripts

$ave,—$ = pitchwise average at a given axial location
$ave,==$ = area average
aw = adiabatic wall
c = coolant conditions
in = inlet value at 1C upstream of blade
ms = value at blade midspan
∞ = local inviscid value
w = wall temperature with heat transfer surface
b = background temperature for surface radiation

References

[1] Lattime, S. B., and Steinetz, B. M., 2002, ''Turbine Engine Clearance Control Systems: Current Practices and Future Directions,'' NASA TM 2002-211794.

[2] Morphis, G., and Bindon, J. P., 1988, ''The Effects of Relative Motioin, Blade Edge Radius and Gap Size on the Blade Tip Pressure Distribution in an Annular Turbine Cascade With Clearance,'' ASME Paper No. 88-GT-256.

[3] Tallman, J., and Lakshmiarayana, B., 2001, ''Numerical Simulation of Tip Leakage Flows in Axial Flow Turbines, With Emphasis on Flow Physics: Part II—Effect of Outer Casing Relative Motion,'' ASME J. Turbomach., **123**, pp. 324–333.

[4] Yaras, M. I., and Sjölander, S. A., 1992, ''Effects of Simulated Rotation on Tip Leakage in a Planar Cascade of Turbine Blades: Part I Tip Gap Flow,'' ASME J. Turbomach., **114**, pp. 652–659.

[5] Mayle, R. E., and Metzger, D. E., 1982, ''Heat Transfer at the Tip of an Unshrouded Turbine Blade,'' *Proc. of 7th Int. Heat Transfer Conf.*, Vol. 3, ASME, New York, pp. 87–92.

[6] Chyu, M. K., Moon, H. H., and Metzger, D. E., 1989, ''Heat Transfer in the Tip Region of Grooved Turbine Blades,'' ASME J. Turbomach., **111**, pp. 131–138.

[7] Srinivasan, V., and Goldstein, R. J., 2003, ''Effect of Endwall Motion on Blade Tip Heat Transfer,'' ASME J. Turbomach., **125**, pp. 267–273.

[8] Kim, Y. W., and Metzger, D. E., 1995, ''Heat Transfer and Effectiveness on Film Cooled Turbine Blade Tip Models,'' ASME J. Turbomach., **117**, pp. 12–21.

[9] Kim, Y. W., Downs, J. P., Soechting, F. O., Abdel-Messeh, W., Steuber, G., and Tanrikut, S., 1995, ''A Summary of the Cooled Turbine Blade Tip Heat Transfer and Film Effectiveness Investigations Performed by Dr. D. E. Metzger,'' ASME J. Turbomach., **117**, pp. 1–11.

[10] Kwak, J. S., and Han, J. C., 2002, ''Heat Transfer Coefficient and Film-Cooling Effectiveness on a Gas Turbine Blade Tip,'' ASME Paper No. GT-2002-30194.

[11] Kwak, J. S., and Han, J. C., 2002, ''Heat Transfer Coefficient and Film-Cooling Effectiveness on a Squealer Tip of a Gas Turbine Blade Tip,'' ASME Paper No. GT-2002-30555.

[12] Acharya, S., Yang, H., Ekkad, S. V., Prakash, C., and Bunker, R., 2002, ''Numerical Simulation of Film Cooling Holes On the Tip of a Gas Turbine Blade,'' ASME Paper No. GT-2002-30553.

[13] Hohlfeld, E. M., Christophel, J. R., Couch, E. L., and Thole, K. A., 2003, ''Predictions of Cooling From Dirt Purge Holes Along the Tip of a Turbine Blade,'' ASME Paper No. GT2003-38251.

[14] Bunker, R. S., Bailey, J. C., and Ameri, A. A., 2000, ''Heat Transfer and Flow on the First-Stage Blade Tip of a Power Generation Gas Turbine: Part 1—Experimental Results,'' ASME J. Turbomach., **122**, pp. 263–271.

[15] Jin, P., and Goldstein, R. J., 2003, ''Local Mass/Heat Transfer on a Turbine Blade Tip,'' Int. J. Rotating Mach., **9**(2), pp. 981–995.

[16] Bindon, J. P., 1989, ''The Measurement and Formation of Tip Clearance Loss,'' ASME J. Turbomach., **111**, pp. 257–263.

[17] Moffat, R. J., 1988, ''Describing the Uncertainties in Experimental Results,'' Exp. Therm. Fluid Sci., **1**, pp. 3–17.

[18] Gnielinski, V., 1976, ''New Equations for Heat and Mass Transfer in Turbulent Pipe and Channel Flow,'' Int. Chem. Eng., **16**, pp. 359–368.

[19] Kakaç, S., Shah, R. K., and Aung, W., 1987, *Handbook of Single-Phase Convective Heat Transfer*, Wiley, New York, pp. 34–35.

[20] Kays, W. M., and Crawford, M. E., 1980, *Convective Heat and Mass Transfer*, Second Edition, McGraw-Hill, New York, pp. 269–270.

[21] Hohlfeld, E. H., 2003, ''Film Cooling Predictions Along the Tip and Platform of a Turbine Blade,'' Master's thesis, Virginia Polytechnic Institute and State University, Blacksburg, VA.

[22] Sen, B., Schmidt, D. L., and Bogard, D. G., 1994, ''Film Cooling With Compound Angle Holes: Heat Transfer,'' ASME Paper No. 94-GT-311.